



# Finite Element Analysis of Cogging Torque and Torque Ripple of Brushless DC Motor

Estabraq A. Abbass<sup>1,\*</sup> and Amer M. Ali<sup>1</sup>

## Affiliations

<sup>1</sup>Department of electrical engineering,  
Mustansiriyah University  
, Baghdad, Iraq

## Correspondence

Estabraq A. Abbass  
[ema2013@uomustansiriya.edu.iq](mailto:ema2013@uomustansiriya.edu.iq)

## Received

15-January-2023

## Revised

01-May-2023

## Accepted

01-August-2024

## Abstract

Brushless DC (BLDC) motors are used in various applications, including industrial, automotive, aerospace, and computers, due to their many benefits. Still, it has some drawbacks, like its cogging torque and torque ripple. A three-phase, 1500-watt, four-pole, inner rotor brushless DC motor was modeled and examined using finite element analysis (FEA) based on Maxwell-2D software to analyze cogging torque at no excitation state and torque ripple at full load condition. Design parameters, including magnet thickness, embrace factor, magnet offset, and initial rotor position, were employed to mitigate their effects on cogging torque and torque ripple. The detailed obtained results will guide BLDC motor designers to select proper values of magnet thickness, embrace factor, offset, and initial rotor position without needing to test many costly produced prototype motors.

Doi: [10.31185/ejuow.Vol12.Iss3.417](https://doi.org/10.31185/ejuow.Vol12.Iss3.417)

**Keywords:** BLDC motor; Cogging torque; Torque ripple; Magnet offset; Magnet thickness; Magnet embrace factor; Initial rotor position; finite element analysis; Maxwell 2D

**الخلاصة:** تُستخدم محركات عديمة الفرش (BLDC) في العديد من التطبيقات، مثل التطبيقات الصناعية والسيارات و أجهزة الفضاء وأجهزة الكمبيوتر، نظرًا لفوائدها العديدة. ولكن لا يزال لديها بعض العيوب، مثل تموج عزم الدوران وعزم الدوران المسنن. تم تصميم محرك DC بدون فرشاة ثلاثي الأطوار، 1500 واط، رباعي الأقطاب، وفحصه باستخدام تحليل العناصر المحدودة (FEA) استنادًا إلى برنامج Maxwell-2D لتحليل عزم الدوران في حالة عدم الإثارة وتموج عزم الدوران في حالة التحميل الكامل. تم استخدام معلمات التصميم، بما في ذلك سماكة المغناطيس، وعامل الطوق، وإزاحة المغناطيس، وموضع الدوار الأولي، للتخفيف من آثارها على عزم الدوران ولغرض تقليل تموج عزم الدوران. ستساعد النتائج التفصيلية التي تم الحصول عليها مصممي محرك (BLDC) لتحديد القيم المناسبة لسماك المغناطيس، وعامل الطوق، والإزاحة، وموضع الدوار الأولي دون الحاجة إلى اختبار العديد من المحركات النموذجية المكلفة المنتجة.

## 1. INTRODUCTION

BLDC motors were improved due to the development of more complex computer technology for control systems. Develops in intelligent electronics and power semiconductors are essential factors that will enhance machine uses in many applications with a wide range of services [1]. The BLDC is split into two types, according to back emf. The back-EMF produced by permanent magnet synchronous motors (PMSM) generally takes the form of sinusoidal waves. In contrast, the back-EMF produced by PMBLDC motors usually takes the shape of a trapezoidal wave [1-3]. Due to the usage of permanent magnets inside the rotor to generate field flux, BLDC motors have substantially lower core and copper losses than conventional DC motors, increasing the overall efficiency of the motor drive system[4]. The BLDC motor has two significant drawbacks: torque ripple and controlling the drives at high speeds. Stator currents are trapezoidal, unlike the quasi-square wave that causes the torque ripple. Torque ripple causes

changes in speed, vibration, and acoustic noise[5]. The cogging torque is present even when the machine is not powered up. It is caused by interactions between the rotor's permanent magnets and the stator winding slots [6]. However, reducing it is usually a significant design priority because it can generate torque ripples and induce vibrations, especially at low speeds and under small loads [7]. Torque ripple results from cogging torque, nontrapezoidal back-emf, and current commutation from one phase to another. Many researchers were interested in analyzing the torque of BLDC motors. Dai used FEM to examine the effects of various variables that affect the torque waveform. It was found that both under-skew and over-skew significantly affect the torque waveform of the BLDC motor[8]. Boukais studied torque ripple and torque with several permanent magnet rotors of BLDC motors. The simulation findings show an influence between this construction, optimal permanent magnet, and optimal segmentation design on the torque ripple[9]. Goutham used Matlab /Simulink to simulate BLDC using a proper controller to reduce torque ripple [10]. Pourjafari found that both cogging torque and torque ripple can be reduced using significant elements such as magnet embrace, offset, and skew[11]. Srisiriwanna investigated the cogging torque reductions of a BLDC motor with varying air gap length, rotor, and stator parts. The finite element method (FEM) is primarily utilized to study torque reduction among these various reduction approaches[12]. Ananthan assesses the magnetic field and motor performance of a (BLDC) motor, the design case with the high electromagnetic torque and the little cogging torque and torque ripple, and presents four design examples with different pole shoe diameters [13]. Dai used FEM to examine the effects of various variables that affect the torque waveform. The experimental data collected under identical conditions validated the computed torque waveforms, and the skew affected the torque waveform[14]. Karthick researched The cogging torque effect by different materials such as; neodymium magnets (NdFeB) and samarium cobalt (SmCo) magnets. The chosen magnetic material will be determined mainly by the application's temperature, device weight, size, and cost[15]. Most of the research studies above examine either the cogging torque or torque ripple of BLDC motors. They also use software tools to accomplish their goals, such as Matlab/Simulink, Maxwell 2D, and Magnet software. The purpose of this research is to simulate and analyze a BLDC motor using Maxwell 2D software and investigate the effect of changing parameters on cogging torque, like magnet thickness, offset, embrace factor at no excitation condition, and the change of the above three parameters on torque ripple, in addition to the initial rotor position at full load condition.

## 2. MATHEMATICAL BACKGROUND

The FEM has excelled in all other electrical motor tools for calculating magnetic fields. Engineers can use it to address problems that are difficult to solve with typical analytical procedures. The approach also allows us to conduct an in-depth analysis of the motor. FEM is a computer-based mathematical approximation method for calculating machine parameters such as torque, induced EMF, flux density, and flux linkage. FEM based on Maxwell 2D software is based on Maxwell's electromagnetic field equations, Which are listed below:[1][4][16].

$$\nabla \cdot D = \rho \quad (1)$$

$$\nabla \cdot B = 0 \quad (2)$$

$$\nabla \cdot E = \frac{-\partial B}{\partial t} \quad (3)$$

$$\nabla \times H = \frac{\partial D}{\partial t} + J \quad (4)$$

Where:

(D) is the electric flux density in ( C.m<sup>-2</sup>)

(ρ) is the volume charge density in (C.m<sup>-1</sup>)

(B) is the magnetic flux density vector term in (Tesla) (E) is the electric field intensity in (V.m<sup>-1</sup>)

(H) is the magnetic field intensity in (A.m<sup>-2</sup>)

The BLDC motor's electromagnetic torque can be expressed as [17]:

$$T_e = \frac{e_a i_a + e_b i_b + e_c i_c}{\omega_m} \quad (5)$$

or

$$T_e = K_t \left[ f(\theta_e) i_a + f\left(\theta_e - \frac{2\pi}{3}\right) i_b + f\left(\theta_e + \frac{2\pi}{3}\right) i_c \right] \quad (6)$$

Where:

(T<sub>e</sub>): is the electromagnetic torque in (N. m)

(K<sub>t</sub>): is the torque constant in (N.m/ A)

The torque ripple can be calculated as [7].

$$\text{Torque ripple (\%)} = \frac{T_{max} - T_{min}}{T_{av}} * 100 \quad (7)$$

Where:

(T<sub>max</sub>): is the maximum value of torque in (N.m).

(T<sub>min</sub>): is the minimum value of torque in (N.m).

(T<sub>av</sub>): is the average torque in ( N. m).

In BLDC motors, cogging torque is the greatest feature affecting the torque ripple. Cogging torque (T<sub>cog</sub>) is caused by the interaction of the rotor-mounted permanent magnet field and the stator teeth, and its equation is shown below [11, 18].

$$T_{cog} = -\frac{1}{2} \phi_g^2 \frac{dR}{d\theta} \quad (8)$$

Where:

(R) is the reluctance of the air gap, (ϕ<sub>g</sub>) is the flux of the air gap, and (θ) is the rotor's angular position [14]

### 3. MODELING OF BRUSHLESS DC MOTOR

RMxprt is a software that uses templates to help electrical machine designers improve their work. RMxprt can determine machine performance and make initial sizing decisions. RMxprt can automatically configure the entire

Maxwell project 2D for transient electromagnetic analysis. Design sheets include a graphic representation of waveforms and a list of all the necessary input and calculated parameters. To determine performance, it combines a magnetic circuit approach with conventional electric machine theory[4].

The finite element method is the numerical strategy for analyzing physics and engineering problems. FEM implies that the machine body is subdivided into smaller pieces and that numerical integration is used for each element [16]. For a three-phase, four poles, inner rotor, 1500 watts. The RMXprt model can generate the 2D –FEM, and reference [19] was adopted for motor specifications and parameters. Since the resistance was meager and the voltage was relatively high for motor derive, chopped current control (CCC), as shown in Figure 1, must be used instead of primary DC control. When using the RMXprt model, the 2D -FEM can be exported to Maxwell 2D. Figure.2 shows the finite element mesh of the analyzed model.

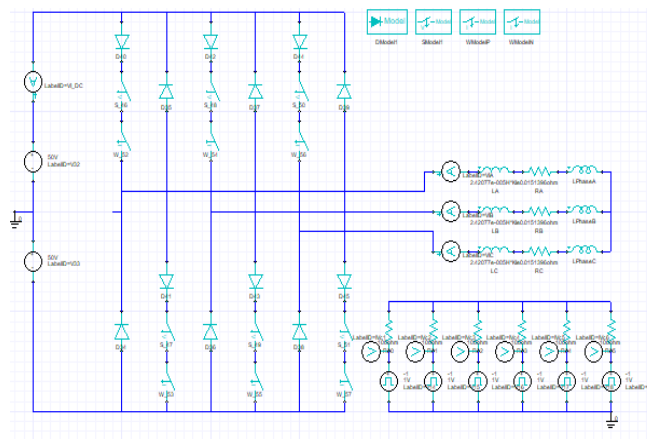


**Fig 1.** External circuit of BLDC motor by Maxwell 2D

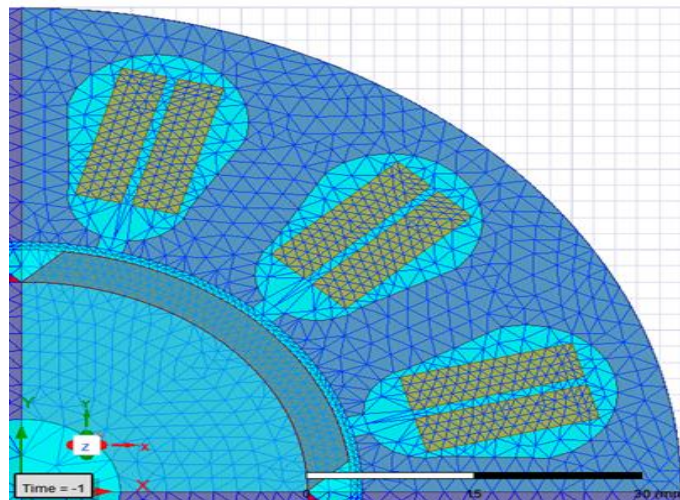


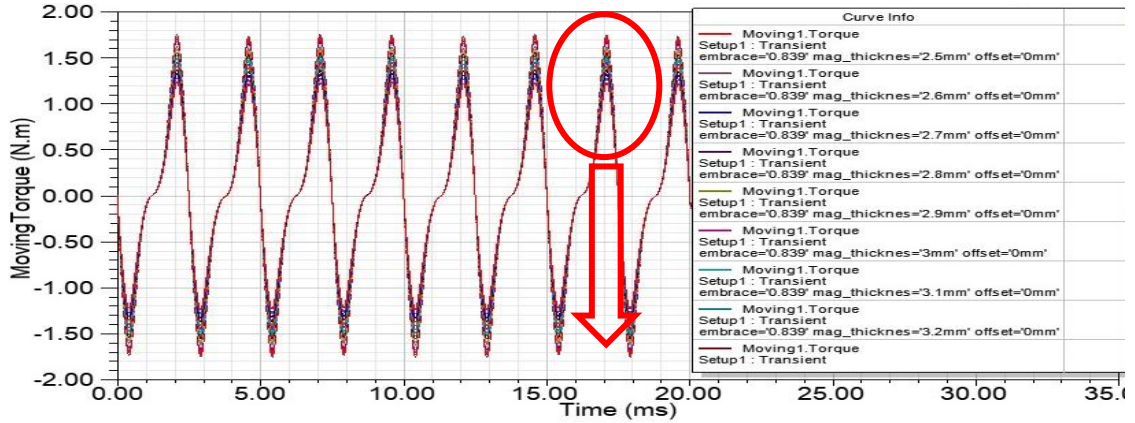
**Fig 2.** Finite element mesh of BLDC motor

#### 4. ANALYSIS OF COGGING TORQUE

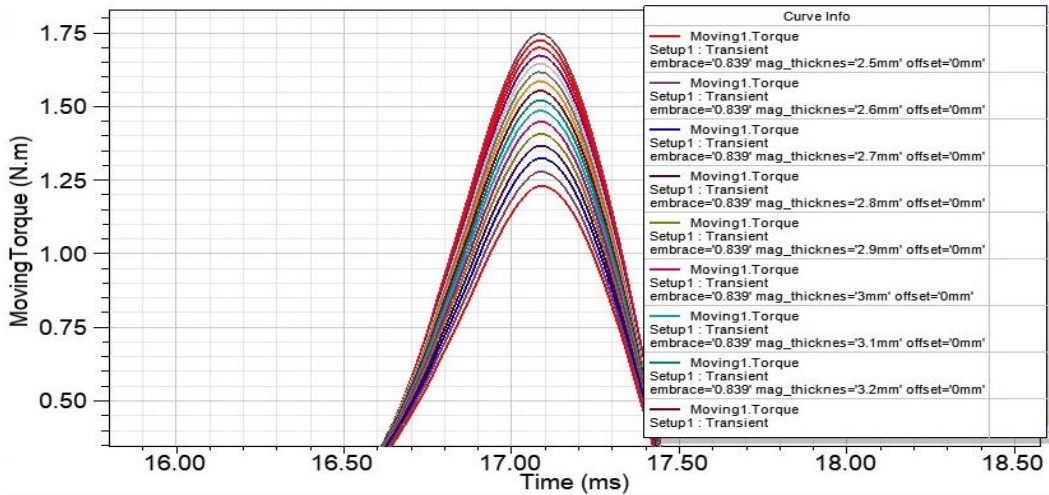
In this paper, three parameters are taken for studying their effects on cogging torque: magnet thickness, embrace factor, offset at no excitation condition, and the same parameters are also studied torque ripple in addition to the initial position at full load. The maximum torque measures the cogging torque at no excitation. Cogging torque analysis is performed using the finite element method based on Maxwell 2D.

### 4.1 Magnet thickness study

This study changed the magnet thickness from 2.5mm to 4mm with a step of 0.1mm. The other parameter is designated as a default value (Embrace factor =0.839, offset=0). Figure (3-a) shows that the average torque is zero at no excitation. The maximum value of cogging torque produced torque in Figure (3-b) shows that the maximum cogging torque was changed by changing magnet thickness when all other parameters were fixed.



(a)



(b)

**Fig. 3.** (a) Average torque of BLDC motor at no excitation vs. magnet thickness (b) zoom of maximum cogging torque

The results of Figure 3 can be represented in Figure 4.

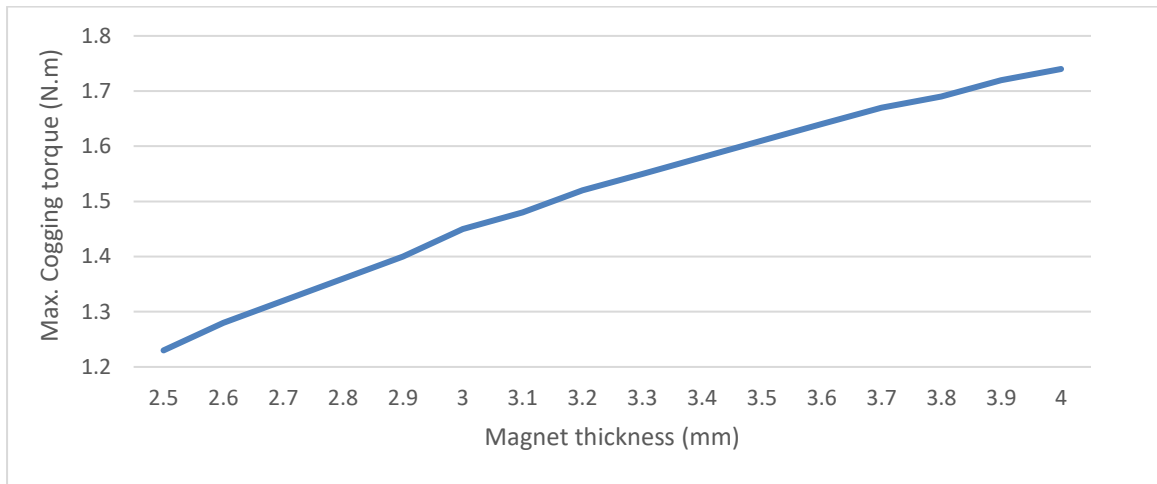
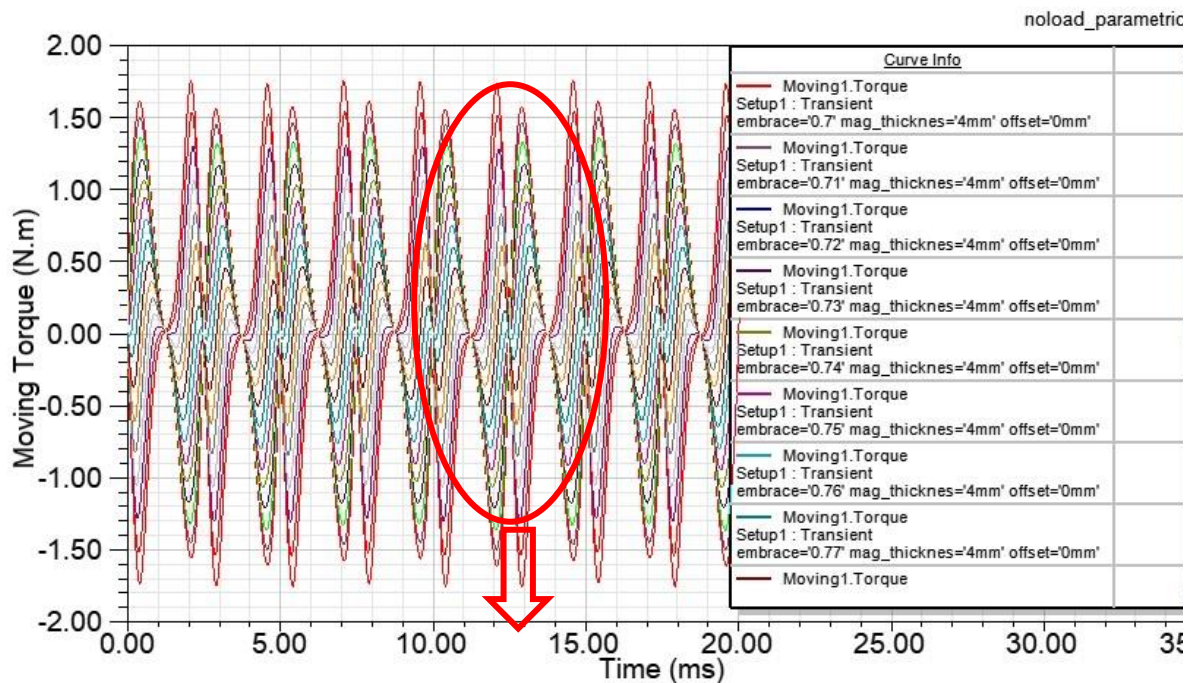


**Fig 4.** Maximum cogging torque vs. magnet thickness

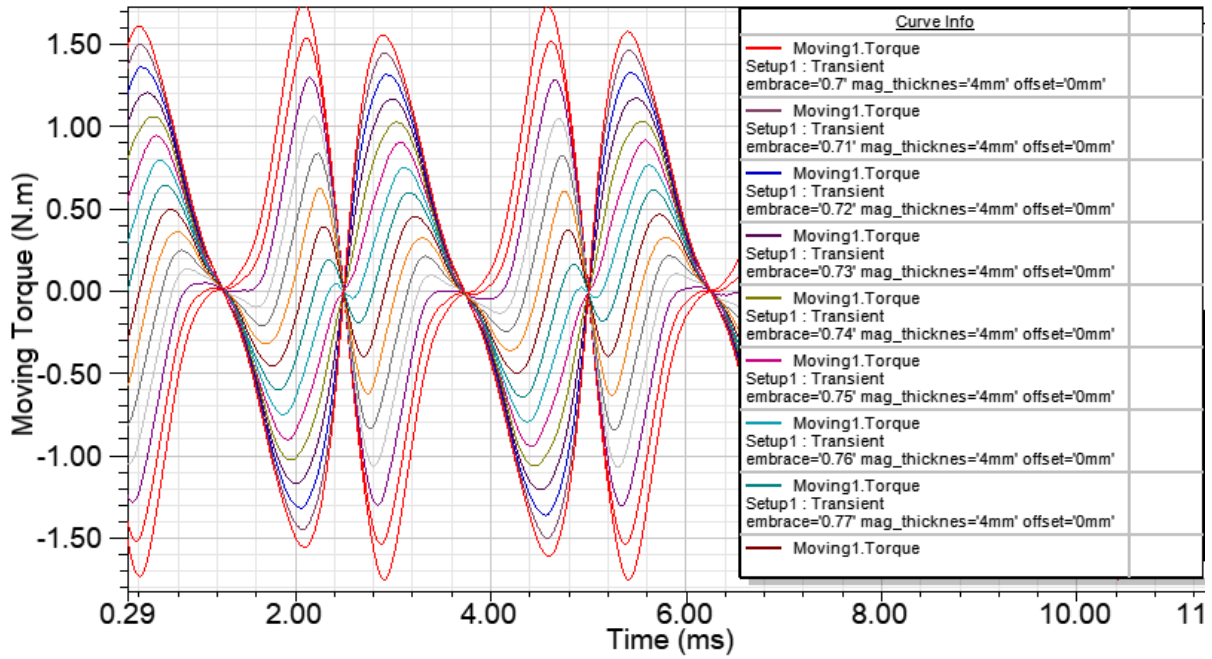
It is evident from the results that the cogging torque will increase ( from 1.32 to 1.74 N.m) in proportion to the magnet thickness (from 2.5 to 4 mm) since the magnetic flux increases with the permanent magnet thickness.

### 4.2 Magnet embrace factor study

The magnet embrace factor is the ratio of the magnet arc to the pole arc. [7]. The parametric technique successfully determines the optimal magnet thickness, just like it did for the optimized embrace value. The magnet embrace factor was changed from 0.70 to 0.84 with 0.01 steps. All the other variables remain fixed in this parametric sweep of Maxwell 2D. (Thickness =4mm, offset=0)With no excitation, the produced torque is cogging torque. Figure 5-a shows that the average torque is zero, and, Figure 5-b shows the cogging torque changes with the change of embrace factor.



(a)



(b)

Fig 5. (a) Average torque of BLDC motor at no excitation vs. embrace factor (b) zoom of maximum cogging torque

The results of Figure 5 can be represented as a chart in Figure 6.

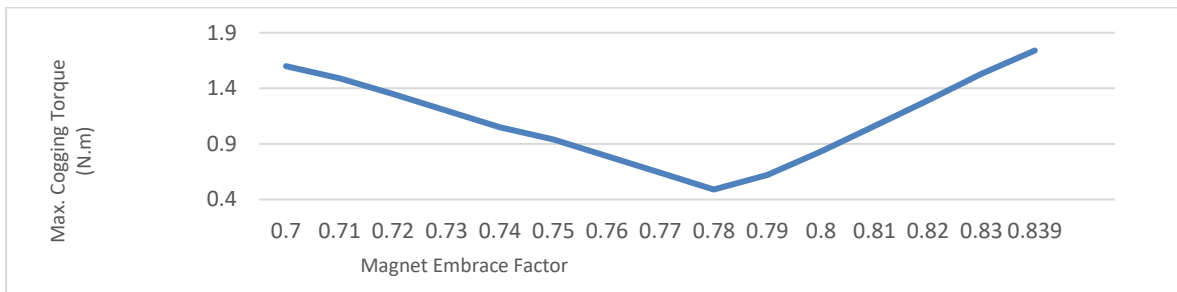


Fig 6. Maximum cogging torque vs. magnet embrace chart

The Figure above shows that the lowest value of maximum cogging torque (0.49 N.m) will happen in the 0.78 embrace factor.

### 4.3 Magnet offset study

Magnet offset is the difference in the rotor's and magnet radii's center. And its effect on the Magnet shape. Air gap flux density is influenced by magnet form. The air gap flux density impacts the torque pulsation, as indicated in[7]. The magnet offset is changed in this paper from 0 to 10 mm with the step of 1mm. Figure 7 shows the shape of the magnet changes with a different offset. 7-a shows the shape with offset =0 mm, figure 7-b shows offset =5mm, and figure 7-c with offset =10mm .Therefore, similar to embrace, various offsets lead to various torque pulsations. In this parametric sweep, the offset was changed, and all the other variables remained fixed. (magnet thickness =4mm, embrace factor =0.839 , rotor initial position= 30 degree).

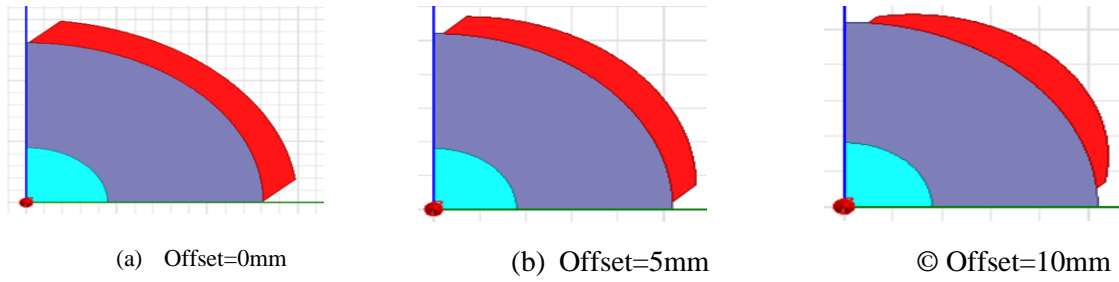
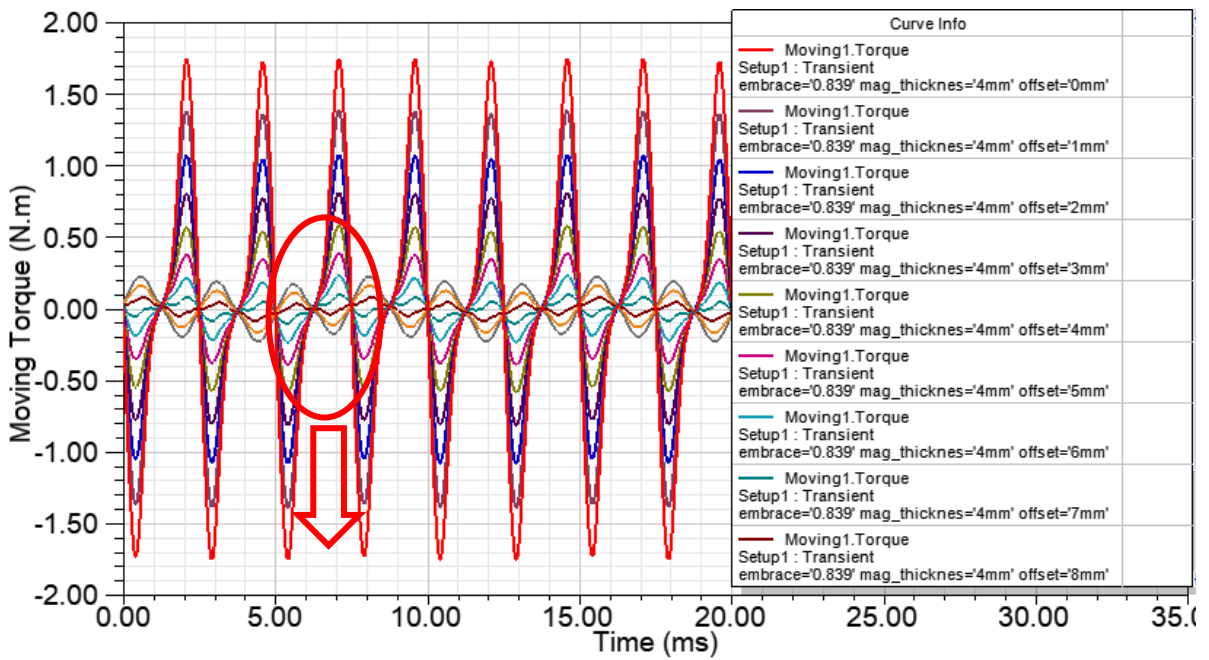
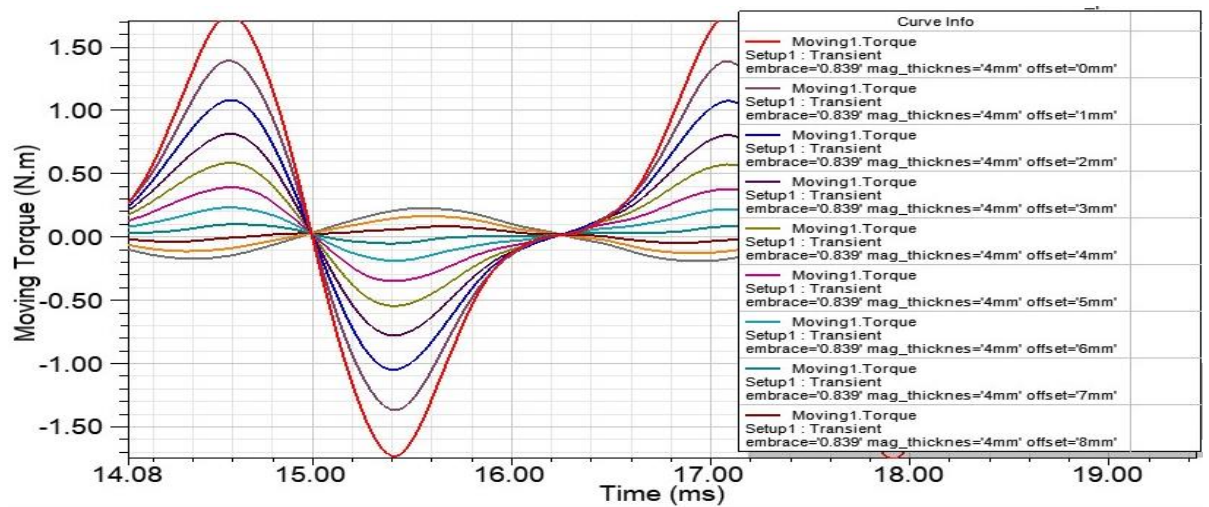


Fig 7. Rotor shape vs. magnet offset

Figure 8-a shows the relation between cogging torque with different values of magnet offset, and Figure 8-b shows the enlarged view of maximum cogging torque.



(a)



(b)

Fig 8. (a) average torque of BLDC motor at no excitation vs. magnet offset factor (b) zoom of maximum cogging torque



Figure 9 shows that the maximum cogging torque decreases by increasing the magnet offset value. Since the primary source of cogging torque is the force interaction between the magnet and the iron teeth, so by increasing the magnet offset value, that leads to decreasing the value of cogging torque. The results of Figure 8 can be represented as a chart of Figure 9.

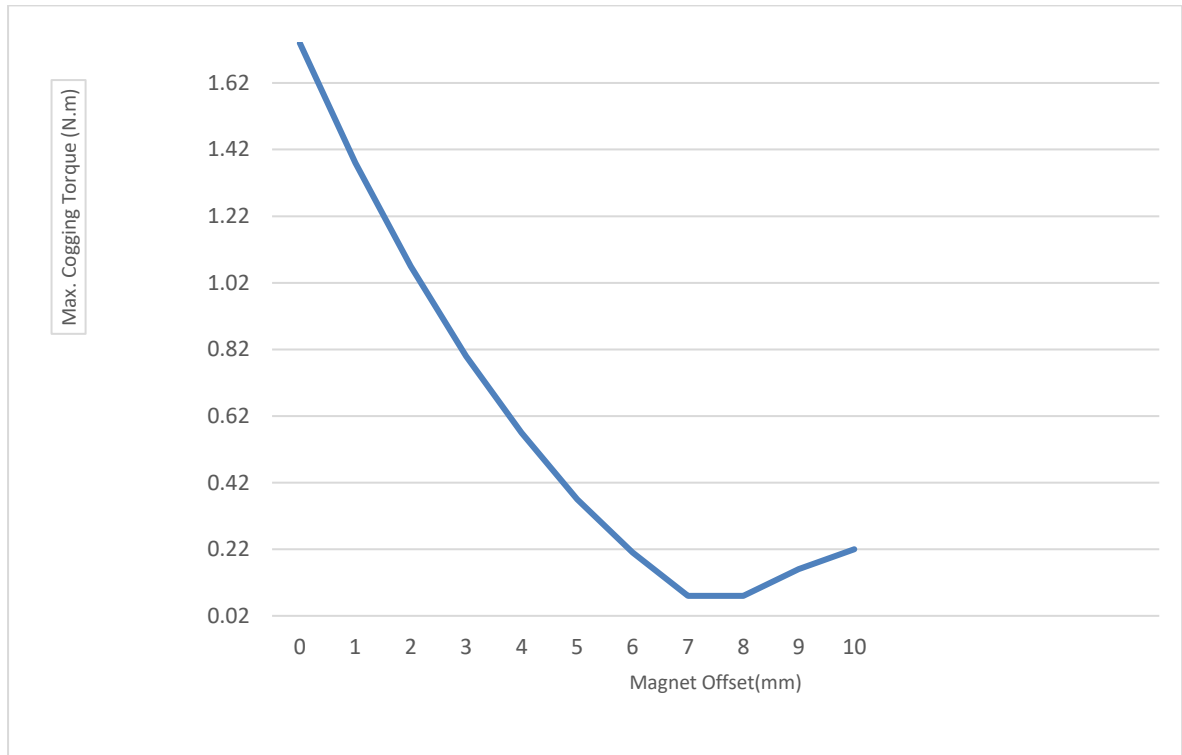


**Fig 9.** Maximum cogging torque vs. offset charts

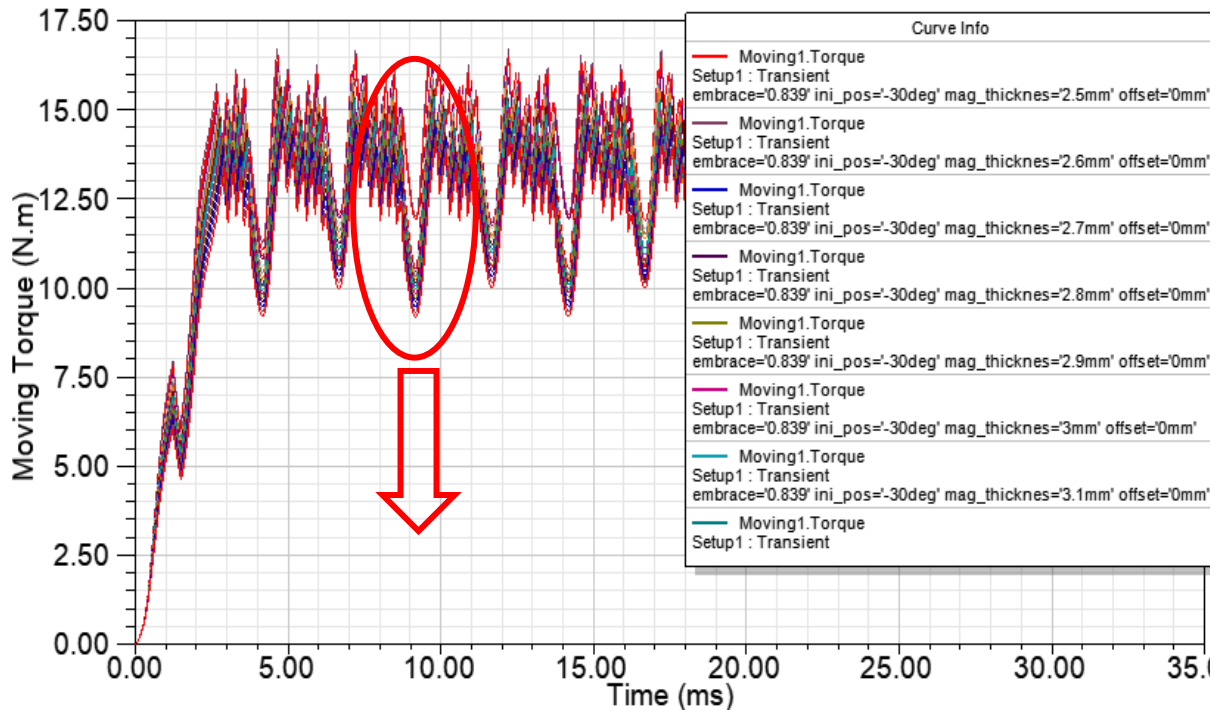
The lowest value of maximum cogging torque (0.08 N.m) happens at a (7 -8) mm offset. After this value, it starts to increase again. This may be due to the decreasing magnet volume with increasing offset values, which will need more research to explore.

## 5. TORQUE RIPPLE ANALYSIS

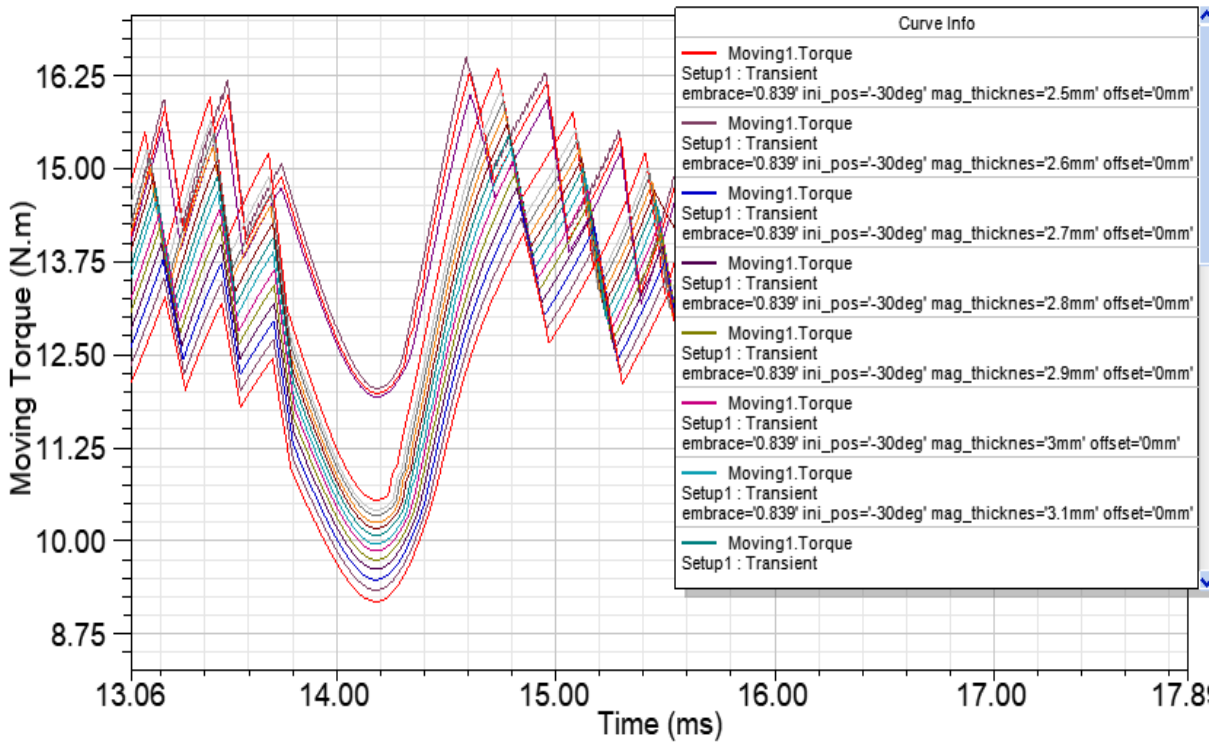
Torque ripple happens in the BLDC motor when it is excited. Four parameters were studied to reduce the torque ripple at full load conditions: magnet thickness, embrace factor, magnet offset, and initial position.

### 5.1. Magnet thickness study at full load

The BLDC motor simulation was done at 2000 rpm. Figure 10 shows the average torque change with changing magnet thickness at full load while the other parameters were fixed.



(a)



(b)

**Fig 10.** (a) average torque of BLDC motor at full load vs. magnet thickness (b) zoom of torque ripple

The result of Figure 10. It can be represented as a chart in Figure 11.

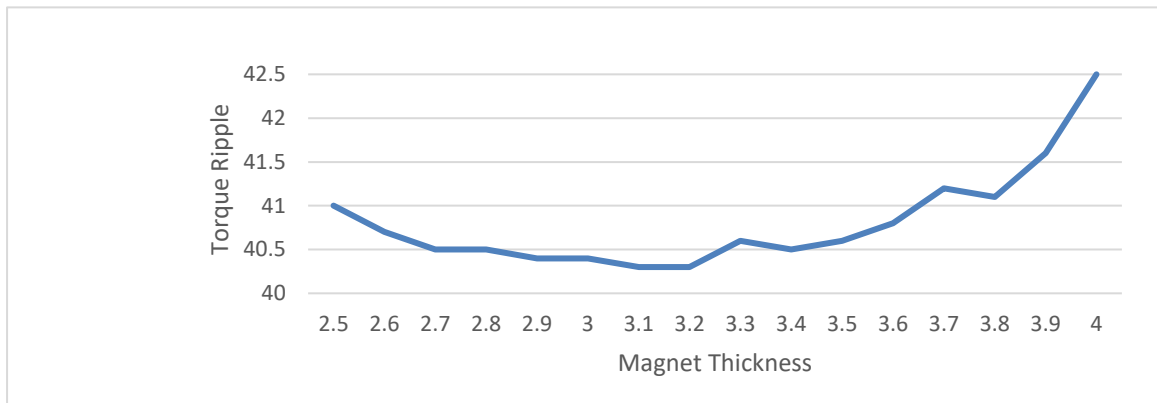
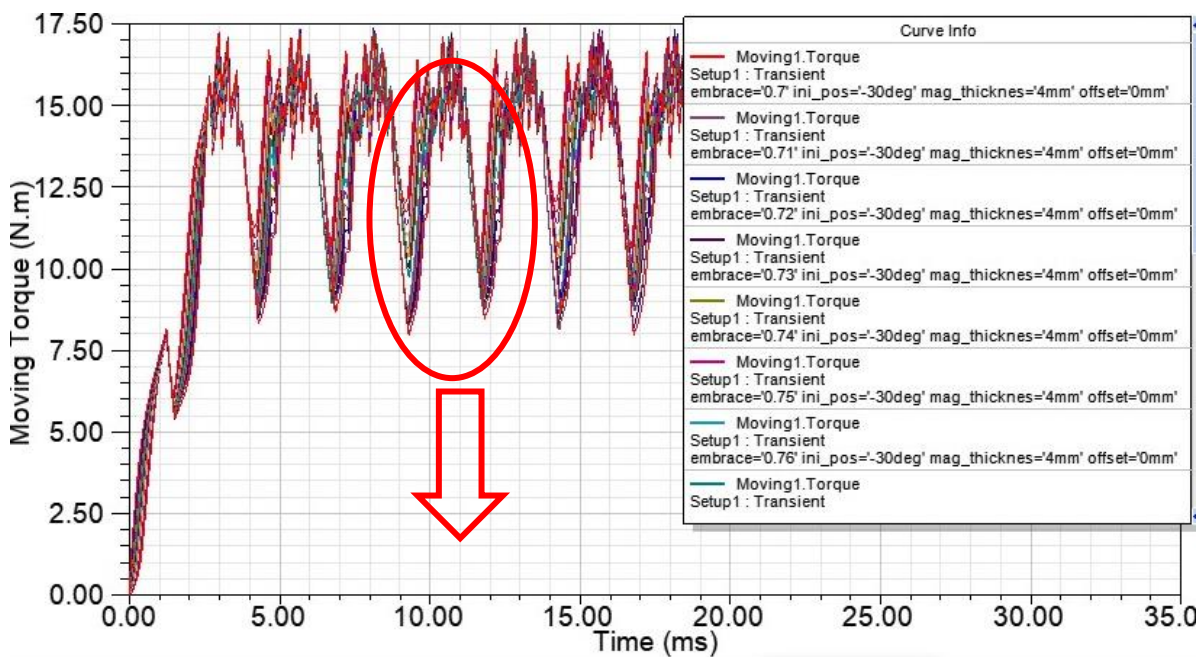


**Fig 11.**Torque ripple vs. magnet thickness at full load

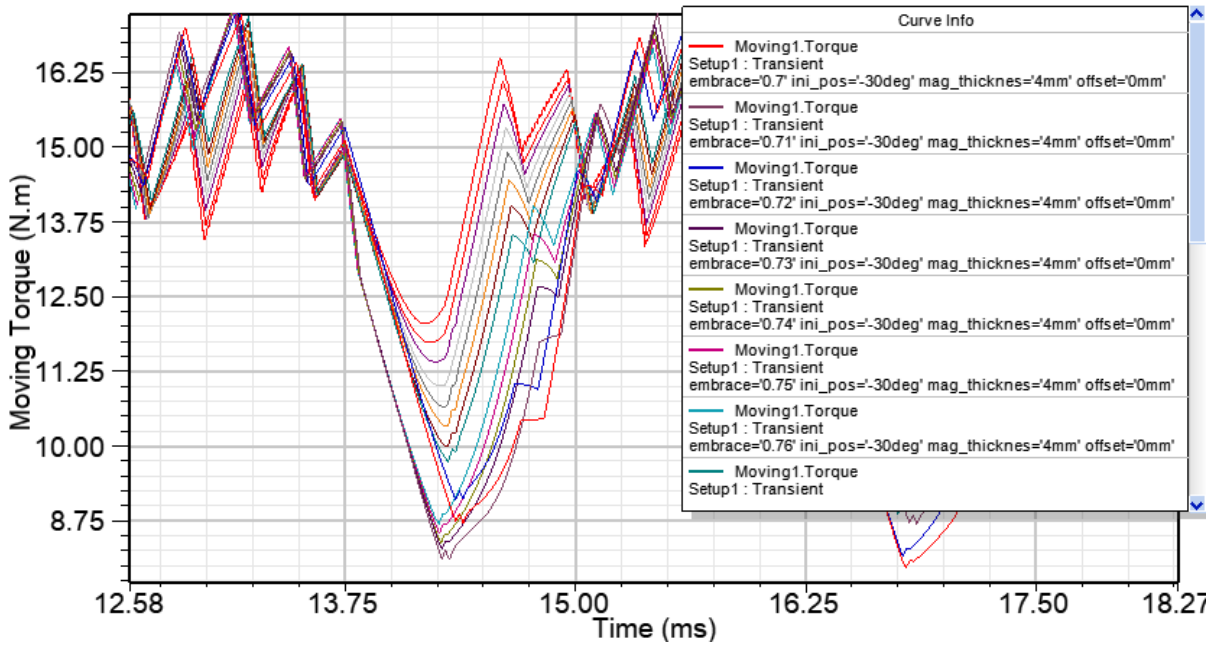
According to the findings, increasing magnet thickness will change the torque ripple due to changing cogging torque with increasing magnet thickness, as studied previously. The magnet thickness has an ideal range from 3.1 to 3.2 mm to produce a minimum value of torque ripple (40.3%).

### 5.2 Magnet embrace factor study at full load

The average torque was calculated, and the results were reported as shown in figure12; the parametric sweep of Maxwell 2D is of magnet embrace from 0.7 to 0.839, and the other parameters were fixed at the initial value



(a)



(b)

**Fig 12.** (a) average torque of BLDC motor at full load vs. embrace factor (b) zoom of torque ripple

Figure 13 shows the torque ripple change with the rotor embrace factor.

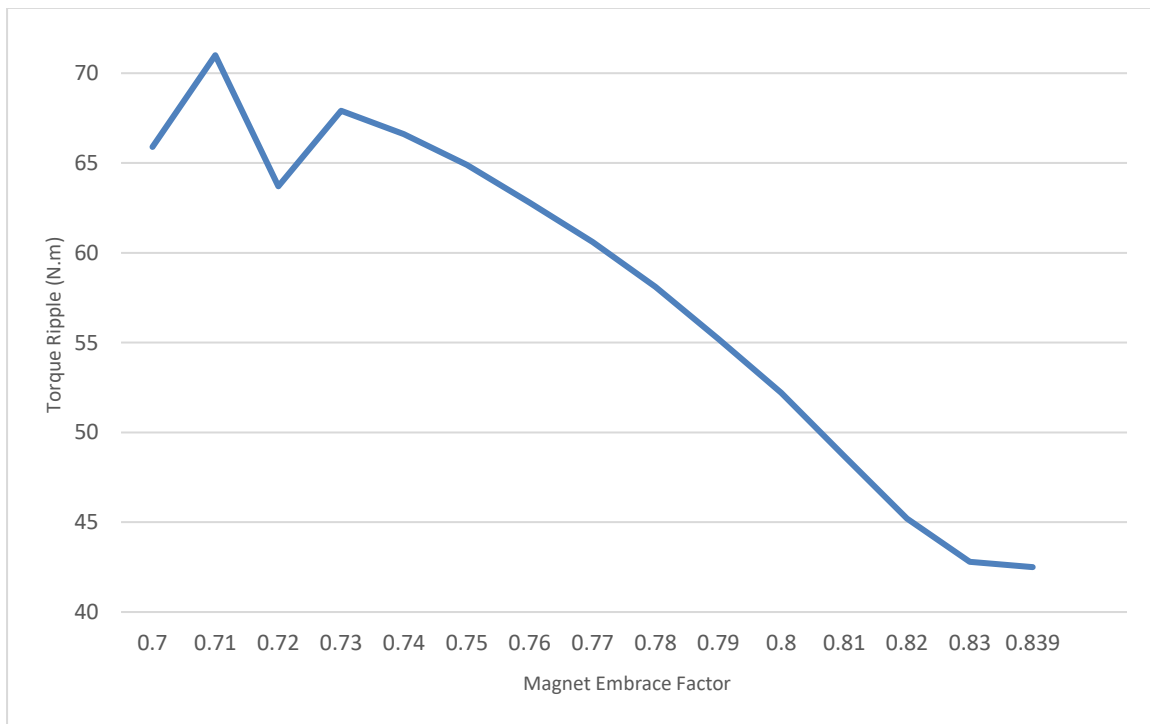
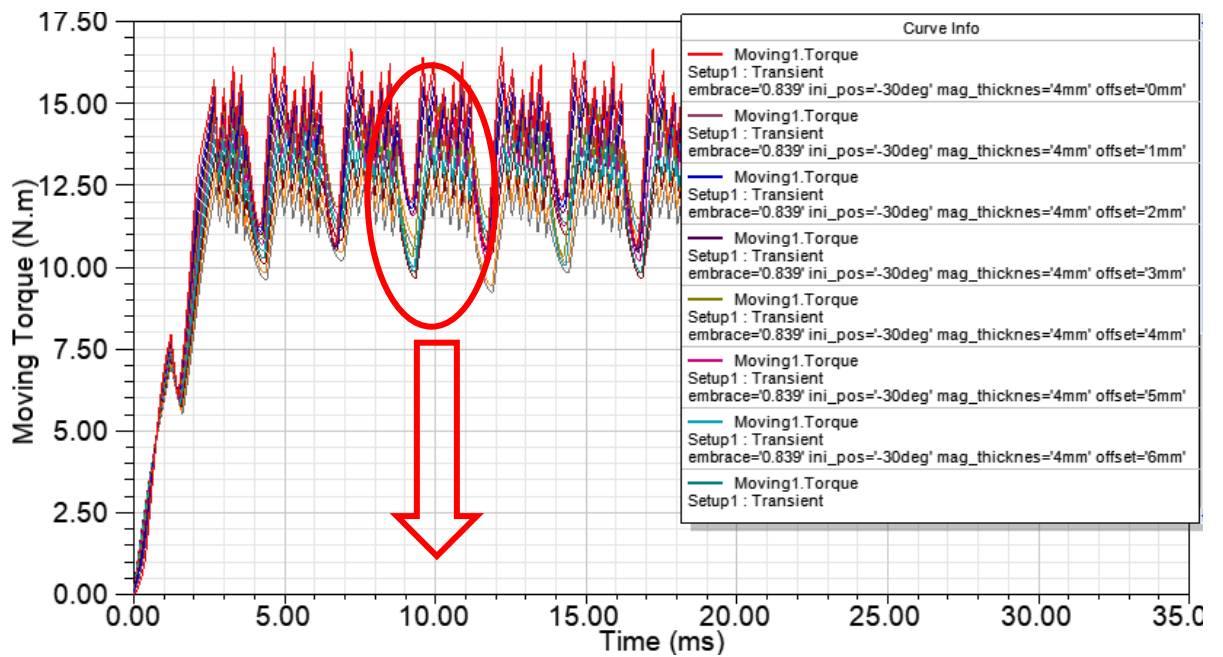


**Fig 13.** Torque ripple vs. embrace factor at full load

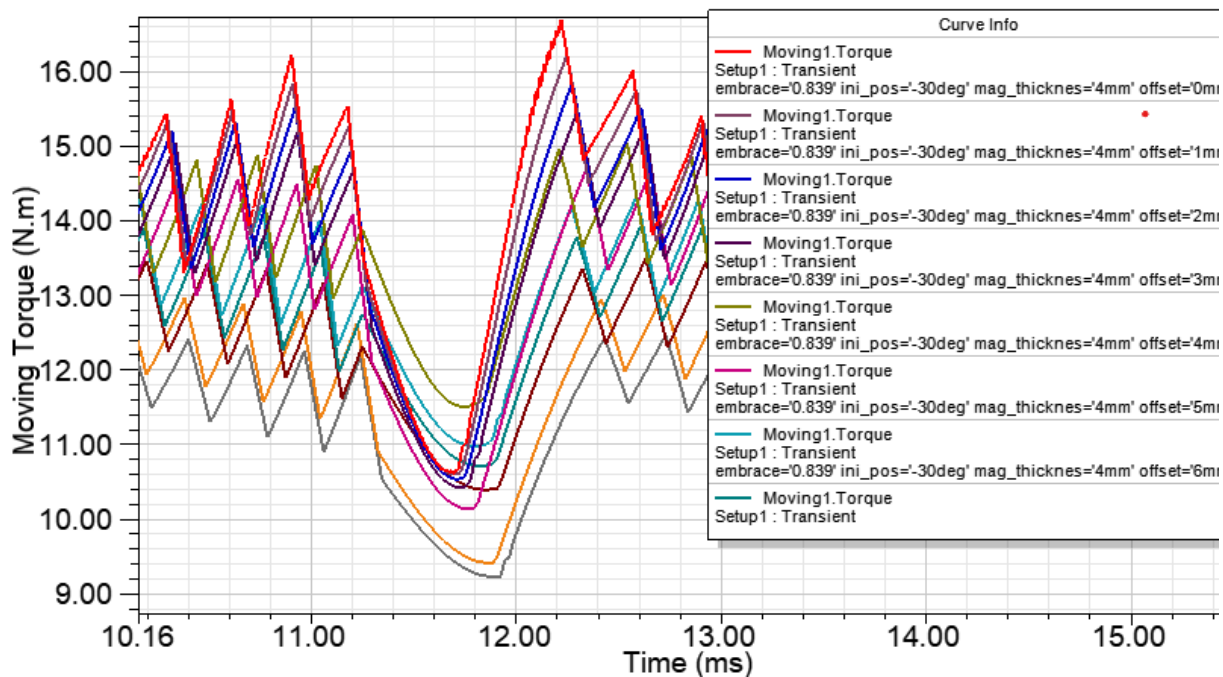
The results show that when the embrace factor increases, the torque ripple was decreased, and the minimum torque ripple (42.5%) happens at the maximum possible embrace factor (0.839).

### 5.3 Magnet offset study at full load

In this case, the torque is calculated, and the results have been reported, as shown in Figure 14. The offset will change from 0 to 10 mm, and the other parameters were fixed.



(a)



(b)

**Fig 14.** (a) Average torque of BLDC motor at full load vs. magnet offset (b) zoom of torque ripple

In Figure 15, the torque ripple vs. offset is shown as a chart

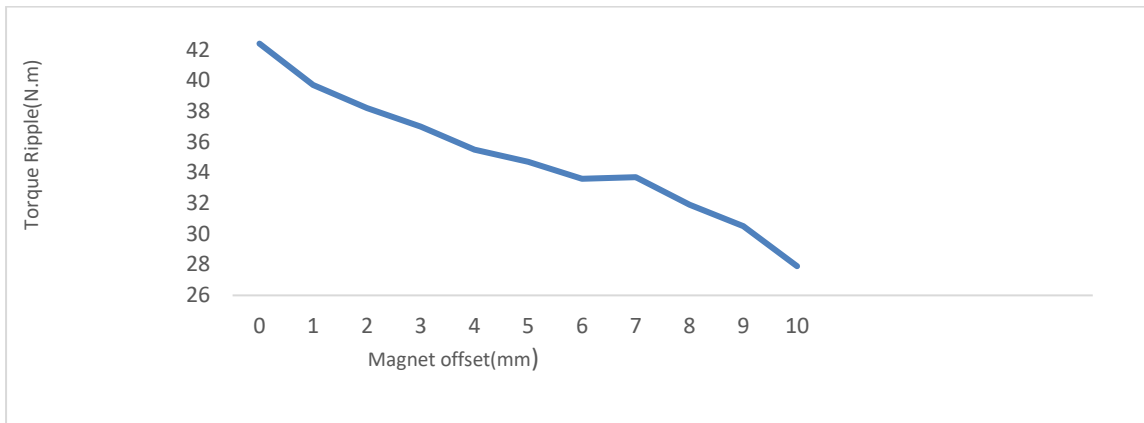
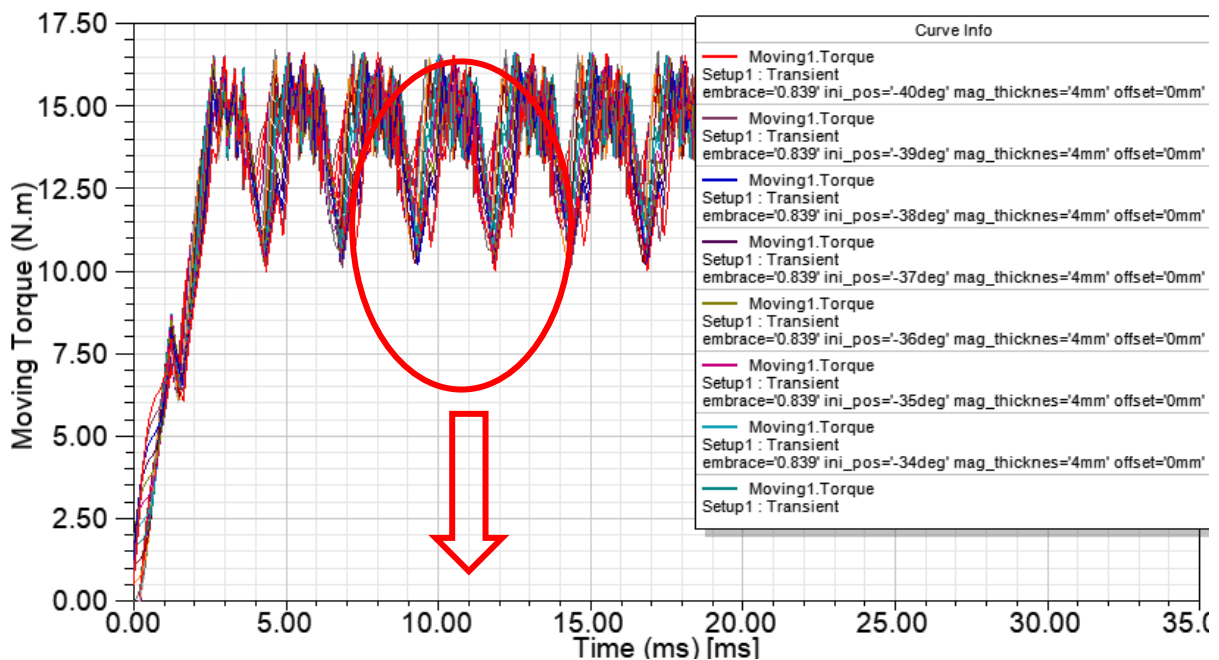


**Fig 15.** Torque ripple vs. offset at full load

The results show that the torque ripple was reduced when the offset increased. The minimum value of torque ripple (27.9%) happens at a magnet offset equal to 10mm.

### 5.4 Rotor initial position study

A three-phase BLDC motor powered by an inverter requires knowledge of the rotor position to achieve stable operation by synchronizing the phase excitation to the rotor position using Hall devices or encoders. Still, the cost is one of the disadvantages. Since a startup is one of the main issues in sensorless BLDC drives, which mostly rely on back-electromotive-force (EMF), the back-EMF voltage disappears at a standstill. However, a short reverse rotation or a startup failure may occur to address the starting issue because of uncertain load characteristics and no initial rotor position [20]. In this section rotor's initial position has been studied. This angle will change the field angle between the rotor and stator field: The angle changed from 25 to 40 degrees with 1 step of degree. The full-Load simulation is presented here, and the torque ripple for each simulation is extracted, as shown in Figure 16. The parametric sweep of Maxwell 2D is for the initial position, and all the other variables remain fixed. ( magnet thickness =4mm, embrace factor=0.839 , offset=0).



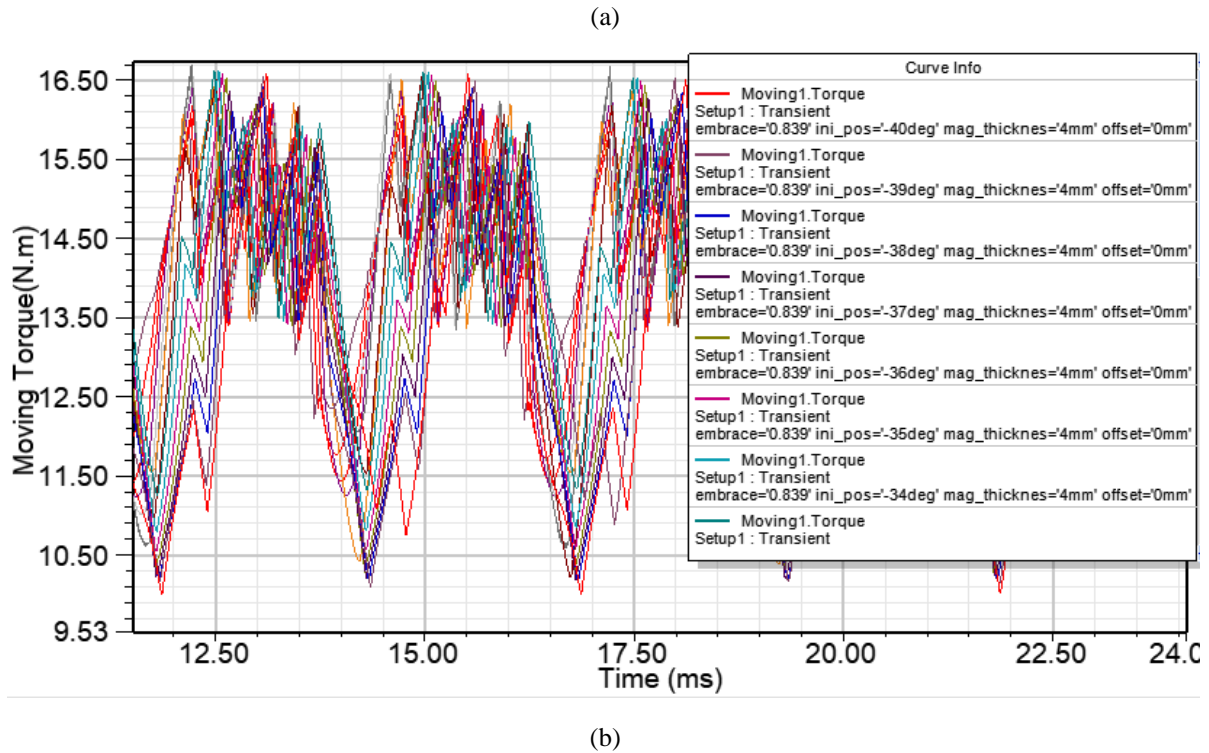


**Fig 16.** (a) Average torque of BLDC motor at full load vs. initial position (b) zoom of torque ripple

In Figure 17, the results were represented as a chart.

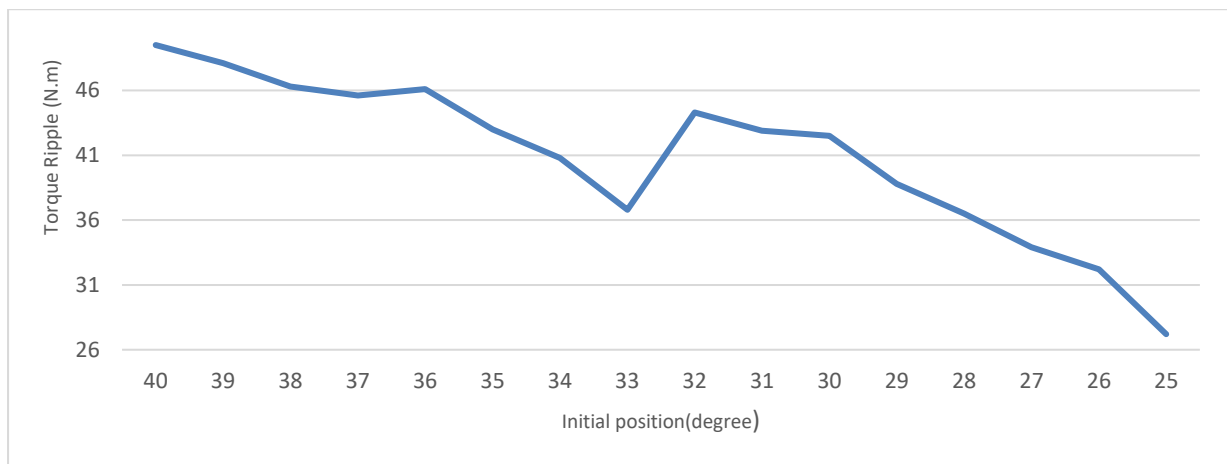


**Fig 17.** Torque ripple vs. initial position at full load

From the above results, changing the rotor's initial position will change the angle between the rotor and the stator field. In this case, the minimum torque ripple (27.2%) happened at 25 degrees of the initial rotor position.

## 6. CONCLUSIONS

A finite element analysis based on Maxwell 2D software is applied to the BLDC motor to study the effect of changing some design parameters, like (magnet thickness, magnet embrace factor, and magnet offset) on motor cogging torque at no excitation condition. And on torque ripple at full load condition with the changing in of initial rotor position. The results showed that the maximum cogging torque produced in the motor is directly proportional to magnet thickness, inversely proportional to magnet offset, and swinging down and up with increasing magnet

embrace factor. The torque ripple swings down and up with increasing magnet thickness and decreases with increasing magnet embrace factor, magnet offset, and initial rotor position. The easiest and cheapest way to reduce torque ripple is by controlling the rotor's initial position. The FEM results from both cogging torque and torque ripple will guide BLDC motor designers to select a good value of magnet thickness, embrace factor, offset, and initial rotor position without needing to produce and test many costly prototype motors. Extra research can be done based on the results obtained to achieve an optimum motor torque.

## ACKNOWLEDGMENT

Thanks, and praise to God Almighty and Majestic first for the blessing of patience and the ability to complete work. The authors would like to thank the Department of Electrical Engineering at the College of Engineering, Mustansiriyah University, for the support and encouragement to complete this research.

## REFERENCES

1. Apatya, Y. B. A., Subiantoro, A., & Yusivar, F. (2017). Design and prototyping of 3-phase BLDC motor. QiR 2017 - 2017 15th International Conference on Quality in Research (QiR): International Symposium on Electrical and Computer Engineering, 2017-Decem, 209–214. <https://doi.org/10.1109/QIR.2017.8168483>
2. Bianchini, C., Immovilli, F., Lorenzani, E., Bellini, A., & Davoli, M. (2012). Review of design solutions for internal permanent-magnet machines cogging torque reduction. *IEEE Transactions on Magnetics*, 48(10), 2685–2693. <https://doi.org/10.1109/TMAG.2012.2199509>
3. Boukais, B., & Zeroug, H. (2010). Magnet segmentation for commutation torque ripple reduction in a brushless DC motor drive. *IEEE Transactions on Magnetics*, 46(11), 3909–3919.
4. Cham, C. L., & Samad, Z. Bin. (2014). Brushless DC motor electromagnetic torque estimation with single-phase current sensing. *Journal of Electrical Engineering and Technology*, 9(3), 866–872. <https://doi.org/10.5370/JEET.2014.9.3.866>
5. Champa, P., Somsiri, P., Wipasuramonton, P., & Nakmahachalasint, P. (2009). Initial rotor position estimation for sensorless brushless DC drives. *IEEE Transactions on Industry Applications*, 45(4), 1318–1324. <https://doi.org/10.1109/TIA.2009.2023355>
6. Dai, M., Keyhani, A., & Sebastian, T. (2001). Torque ripple analysis of a permanent magnet brushless DC motor using finite element method. *IEMDC 2001 - IEEE International Electric Machines and Drives Conference*, 19(1), 241–245. <https://doi.org/10.1109/IEMDC.2001.939306>
7. Goutham, R., Raju, G., Powl, S. J., Sathishkumar, A., & Sivaprakasam, P. (2012). Mitigation of Torque for Brushless DC Motor: Modeling and Control. *International Journal of Scientific & Engineering Research*, 3(5). <http://www.ijser.org>
8. He, C., & Wu, T. (2016). Design, analysis, and experiment of a permanent magnet brushless DC motor for electric impact wrench. *Proceedings - 2016 22nd International Conference on Electrical Machines, ICEM 2016*, 1591–1597. <https://doi.org/10.1109/ICELMACH.2016.7732736>
9. J. Kazem, A., & M. Ali, A. (2021). Finite Element Analysis of Shaded Pole Motor Based on Maxwell2D. *Journal of Engineering and Sustainable Development*, 25(Special), 1-115-1–220. <https://doi.org/10.31272/jeasd.conf.2.1.25>
10. Kanapara, A. J., & Badgujar, K. P. (2020). Performance improvement of permanent magnet brushless DC motor through cogging torque reduction techniques. *2020 21st National Power Systems Conference, NPSC 2020*, 1–6. <https://doi.org/10.1109/NPSC49263.2020.9331855>
11. Karthick, K., Ravivarman, S., Samikannu, R., Vinoth, K., & Sasikumar, B. (2021). Analysis of the Impact of Magnetic Materials on Cogging Torque in Brushless DC Motor. *Advances in Materials Science and Engineering*, 2021. <https://doi.org/10.1155/2021/5954967>
12. Kumar, A., Gandhi, R., Wilson, R., & Roy, R. (2020). Analysis of Permanent Magnet BLDC Motor Design with Different Slot Type. *2020 IEEE International Conference on Power Electronics, Smart Grid and Renewable Energy, PESGRE 2020*, 1–6. <https://doi.org/10.1109/PESGRE45664.2020.9070532>
13. Kumar, P., Bhaskar, D. V., Behera, R. K., & Muduli, U. R. (2020). A modified torque ripple minimization technique for bldc motor drive using synthesized current phase compensation. *Proceedings of the IEEE International Conference on Industrial Technology*, 2020-Febru, 127–132. <https://doi.org/10.1109/ICIT45562.2020.9067134>
14. Lee, T. Y., Seo, M. K., Kim, Y. J., & Jung, S. Y. (2016). Motor Design and Characteristics Comparison of Outer-Rotor-Type BLDC Motor and BLAC Motor Based on Numerical Analysis. *IEEE Transactions on Applied Superconductivity*, 26(4). <https://doi.org/10.1109/TASC.2016.2548079>



15. N, A., N, V., & A, G. kumar. (2015). Design and Analysis of Brushless D . C Motor for Reduce Cogging Torque Using. 1(1), 35–41.
16. Patel, D. M., Makwana, U. L., & College, L. D. (2017). Finite Element Analysis of Permanent Magnet Brushless DC Motor. *International Research Journal of Engineering and Technology (IRJET)*, 4(4), 1835–1838. <https://www.irjet.net/archives/V4/i4/IRJET-V4I4383.pdf>
17. Pourjafari, M., Choolabi, E. F., & Jafarboland, M. (2012). Optimum Design of Brush- Less DC Motor with Minimum Torque Pulsation Using FEM & PSO. 44(2), 59–70.
18. Srisiriwanna, T., & Konghirun, M. (2012). A study of cogging torque reduction methods in brushless DC motor. 2012 9th International Conference on Electrical Engineering/Electronics, Computer, Telecommunications and Information Technology, ECTI-CON 2012, 0–3. <https://doi.org/10.1109/ECTICon.2012.6254191>
19. Vipin Kumar Singh, Prof. Sanjay Marwaha, & Ashish Kumar Singh. (2017). Design and Analysis of Permanent Magnet Brushless DC Motor for Solar Vehicle using Ansys Software. *International Journal of Engineering Research And*, V6(04), 1215–1220. <https://doi.org/10.17577/ijertv6is040795>
20. Zhu, Z. Q., & Howe, D. (2000). Influence of design parameters on cogging torque in permanent magnet machines. *IEEE Transactions on Energy Conversion*, 15(4), 407–412. <https://doi.org/10.1109/60.900501>